Environmental Technology & Innovation 28 (2022) 102940

Contents lists available at ScienceDirect

Environmental Technology & Innovation

journal homepage: www.elsevier.com/locate/eti

Optimization of the synthesis of activated carbon prepared from *Sargassum (sp.)* and its use for tetracycline, penicillin, caffeine and methylene blue adsorption from contaminated water

Marckens Francoeur [a,b,*], Christelle Yacou [a], Corine Jean-Marius [a], Yvens Chérémond [b], Ulises Jauregui-Haza [c], Sarra Gaspard [a]

[a] *Laboratory COVACHIM-M2E, EA 3592 Université des Antilles, BP 250, 97157 Pointe à Pitre Cedex, Guadeloupe*
[b] *URE, Université d'État d'Haïti, Port-au-Prince, Haiti*
[c] *Instituto Tecnológico de Santo Domingo, Dominican Republic*

ARTICLE INFO

Article history:
Received 21 June 2022
Received in revised form 7 October 2022
Accepted 13 October 2022
Available online 21 October 2022

Keywords:
Sargassum (sp)
Adsorption
Antibiotics
Caffeine
Methylene blue
Activated carbon

ABSTRACT

This study was carried out to determine the optimal conditions for synthesizing activated carbon (AC) derived from invasive *Sargassum (sp)* for the efficient adsorption of emerging micropollutants [i.e. caffeine (Caf), tetracycline (Tc), penicillin V (Pen) and methylene blue (MB)] in wastewaster. A three factor's Doehlert design at two levels (i.e. temperature of pyrolysis, T, mass ratio between activating agent H_3PO_4/ Sargassum, r; and time of pyrolysis, t) and response surface methodology were used. Responses measured for optimization were as follows: production yield, specific surface area, acid and basic groups, point of zero charge and adsorption capacities of Caf, Tc, Pen and MB. For individual systems (pollutants tested separately), optimized AC prepared with predicted parameters (i.e. $T = 664$ °C, $r = 2.4$, $t = 65$ min), has reached adsorption capacities values of 329, 580, 150 and 222 mg g^{-1} for Caf, Tc, Pen and MB, respectively For the quaternary systems (all four micropollutants added simultaneously), total elimination using 200 mg L^{-1} of each molecule was: 39.9%, 48.9%, 39.7% and 70.8% for Caf, Tc, Pen and MB, respectively. These results open a very promising and efficient way for the valorization of *Sargassum (sp)* into AC for elimination of organic pollutants from polluted water.

1. Introduction

The presence of organic and persistent compounds in surface waters and wastewaters is of universal concern. The use of antibiotics has increased continuously during these decades, either for prophylaxis or for the treatment of people, animals and plants (Carvalho and Santos, 2016; Phoon et al., 2020). Between 25 and 75% of these recalcitrant bio accumulative pharmaceuticals compounds that are excreted after ingestion (Homem and Santos, 2011; Rivas et al., 2011), have been detected in several waters and soils (Phoon et al., 2020; Wang et al., 2019). The presence of antibiotics in the environment,

* Corresponding author at: Laboratory COVACHIM-M2E, EA 3592 Université des Antilles, BP 250, 97157 Pointe à Pitre Cedex, Guadeloupe.
E-mail addresses: Marckens.Francoeur@etu.univ-antilles.fr (M. Francoeur), christelle.yacou@univ-antilles.fr (C. Yacou), corine.jean-marius@univ-antilles.fr (C. Jean-Marius), cheryvens@yahoo.fr (Y. Chérémond), ulisesjhaza@yahoo.com (U. Jauregui-Haza), sarra.Gaspard@univ-antilles.fr (S. Gaspard).

https://doi.org/10.1016/j.eti.2022.102940

even at very low concentrations, increases the bio-resistance of bacteria (Tayo et al., 2018; Chaturvedi et al., 2021), which can only be reduced by the complete elimination of these molecules (Levy and Bonnie, 2004). Beside antibiotics, textile dyes (pollutants considered as toxic, mutagenic and carcinogenic) (Ahmed et al., 2015) and other emerging pollutants such as caffeine, are also released into water. Consequently, there is no doubt that the discharge of such chemical products requires innovative but also effective treatment solutions. In fact, as regulation become more stringent, there have been many advances in research to eliminate these pollutants (Ali et al., 2018; Krasucka et al., 2021; Ma et al., 2020; Mansas et al., 2020; Krishnan et al., 2021; Anon, 2021), but there were also among these methods those which have generated other dangerous products or intermediates (Capodaglio, 2020). However, adsorption on activated carbon (AC) is until now a very applicable method due to its simplicity, low manufacturing cost, reusability and due to the assurance of not producing secondary contaminants (Beltrame et al., 2018).

Spearheaded by the recent inundations of *Sargassum (fluitans and natans)* seaweeds along coastal shores, interest in finding reliable recovery routes for these algae has emerged. Indeed, massive influx of these blooms has exploded since 2011 (mainly in coastlines of Brazil, Caribbean, Gulf of Mexico and Western Africa), causing numerous economic disruptions in the tourism and fishing sectors and raising environmental concerns (Pinteus et al., 2018). Consequently, *Sargassum (sp.)* has been investigated as a biosorbent material, for its alginate extraction and as a precursor for the preparation of AC for water treatment (Barquilha et al., 2019; de S. Coração et al., 2020; Esmaeili et al., 2010; Francoeur et al., 2021; Li et al., 2017; He and Chen, 2014). AC prepared from *Sargassum (sp.)* was recently developed in our group to remove caffeine molecules from water (Pinteus et al., 2018). Reasonable removal values were obtained in tandem with a proposed adsorption mechanism via molecular modeling. However, such AC synthesis thus far follows only one preparation condition, which therefore warrants further research to better understand and enhance the adsorption performance.

In the same perspective of contributing to reduce the negative impact of *Sargassum* (*sp.*) on the environment, this study (i) focuses on valorizing the seaweed for the production of AC while trying (ii) to optimize production parameters to increase as much as possible AC adsorption capacity.

For this purpose, four molecules were chosen: caffeine as an emerging pollutant, tetracycline and penicillin V as antibiotics and methylene blue as dye. Design of experiments and response surface methodology were used to define the optimal conditions for the production of an AC with the highest adsorption efficiency for each of those molecules. In that regard, the influence of three main factors (i.e. temperature of pyrolysis, T; mass ratio between activating agent/Sargassum, r; and time of pyrolysis, t) in the synthesis procedure was evaluated. Subsequently, adsorption isotherms were obtained for modeling response surface, the validation of these models was assessed by comparing experimental to predicted values and competitive adsorption of the four molecules was also performed on optimum AC.

2. Material and methods

2.1. Chemicals

Tetracycline (Tc, purity $\geq$ 88%, Lot. 059M4037V), penicillin V potassium salt (Pen, purity $\geq$ 98%, Lot. BCBX3916), caffeine (Caf, purity $\geq$ 98.5%, Lot. 021M0092V) were purchased from Sigma-Aldrich and pure methylene blue (MB, Lot. 310 95-7) from RAL Reagents. *Sargassum (sp)* was collected along the beaches of Guadeloupe (French West-Indies). All other chemical reagents of the study such as H_3PO_4 (85 wt%), NaOH and HCl have an analytical quality.

2.2. Experimental design

Doehlert's plan, proposed by David H. Doehlert in 1970, is used to generate points uniformly but also allows a sequential approach of the response surface (Franco, 2008). An experimental plan with three factors may be perfectly suitable for second-degree response surfaces in the case of response optimization. The results will be used to study the individual and collective influence of these three factors through the responses by variance analysis. Seventeen tests with three center points were carried out (Table A.1). The range of factor levels was chosen accordingly to preliminary studies on the precursor *Sargassum (sp.)* (Francoeur et al., 2021). For the different synthesis, other factors such as N_2 flow of pyrolysis, chemical agent concentration, heating rate and impregnation time were set at 80 mL/min, 85 wt%, 10 °C/min and 15 h, respectively (Francoeur et al., 2021).

The mathematical model of the second degree of prediction was used Eq. (1):

$$Y = \beta_0 + \sum_{i=1}^{3} \beta_i x_i + \sum_{i=1}^{3} \beta_{ii} x_i^2 + \sum_{i<j}^{3} \beta_{ij} x_i x_j \quad (1)$$

where Y is the prediction of the response (adsorption capacity of AC); β_0 is the model constant; β_i, β_{ii} and β_{ij} are the regression coefficients; x_i, x_j are the factors considered. The quality of the model was verified with the calculation of the correlation coefficient R^2 and R^2 adjusted.

Both, the analysis of variance (ANOVA) and response surface curves, which were performed on Ellistat version 6.4 2020/11 and Design expert 13 trial; were used to determine the importance of each coefficient in the responses at 95% confidence level.

Table 1
Detailed parameters of adsorption measurements.

	Caf (20 ml)	Tc (25 mL)	Pen (10 mL)	MB (20 mL)
Mass of AC	15 mg	10 mg	15 mg	15 mg
Initial pH	6.4	5.3	5.6	–
Contact time[a]	3 h	3 h	12 h	3 h

[a]All contact times were fixed after kinetics study of the AC.

Fisher distribution (F-value) and null-hypothesis test (*p*-value) were used to determine the significance of the regression model. A high F-value suggests a better fit of the model. A *p*-value < 0.05 indicates the design variable of a model contributing less than 5% change in the response. Therefore, the variable with the higher F-value and p < 0.05 was considered significant (Radaei et al., 2014). After elimination of non-significant terms, the selected coefficients were used to define the quadratic models for adsorption of each molecule and for the plotting of response surfaces.

Once the quadratic models have been determined and validated for each response, the global desirability function (D) in Eq. (2), which takes into account the requirements of each response, allowed the simultaneous optimization of all modeled responses using a multilinear regression (Mathieu and Phan-Tan-Luu, 2001). Herein, the relative weight of antibiotics was higher than the relative weight of the other two molecules, in order to further optimize the adsorption of antibiotics on AC.

$$D = d_1^{w_1} d_2^{w_2} \dots d_n^{w_n} \qquad \text{with} \qquad \sum_{i=1}^{n} w_i = 1 \tag{2}$$

where d_i is the individual desirability of each response and w_i being the relative weight given to each response.

2.3. Preparation of activated carbon (AC)

The collected *Sargassum (sp.)* were washed, air-dried during one week, oven-dried at 80 °C for 24 h and finally crushed and sieved at 0.4 to 1 mm. AC were prepared by chemical activation of Sargassum with H_3PO_4 using different impregnation mass ratios (g H_3PO_4/ g biomass) varying from 0.5 to 2.5; different pyrolysis times varying from 60 to 120 min and different pyrolysis temperatures varying from 600° to 800 °C (Table A.1). Pyrolysis was carried out in a tube furnace (CARBOLITE GERO CTF 12/95/550) under an inert atmosphere (nitrogen). The resulting ACs were washed with NaOH (0.5 M) up to pH 6 and then with distilled water at 80 °C to a pH close to 7. Finally, samples were dried, ground, sieved at 90 μm and then properly stored for later use.

2.4. Determination of adsorption capacities of micropollutants on AC

Considering adsorption capacity (q_e, mg/g) as the main response variable of the experimental design, adsorption isotherms were determined for each molecule with the obtained AC. (Table A.1). Stock solutions of Caf, Tc, Pen and MB were prepared in distilled water with concentrations varying from 200–5000, 30–650, 20–200 and 150–400 mg L^{-1}, respectively. These concentration ranges were chosen taking into account the solubility of each pollutant in water at 25 °C. Then, an appropriate amount of AC was mixed with one of the solutions placed in closed bottles that were stirred in a thermostated water bath (GFL 1086, 200 rpm, 25 °C). Detailed parameters used in the procedure are given in Table 1. After adsorption, the samples were filtered through a 0.45 μm membrane and analyzed by UV–vis spectrophotometry (UviLine 9400) to determine remaining concentrations of each pollutant. Maxima absorbance wavelengths were identified at 273, 358, 206 and 663 nm for Caf, Tc, Pen and MB, respectively. Those experiments were repeated at least three times with an average experimental variation less than 5%.

2.5. Adsorption studies of the optimum activated carbon (AC_OP)

After identifying optimal preparation conditions based on the results of surface response, an AC (herein referred to as AC_OP) was prepared and further tested with Caf, Tc and Pen in the following experimental ranges of parameters: (i) kinetics (5 min–48 h); (ii) pH (2–10); (iii) temperature (25–40 °C); (iv) adsorption isotherm at 25 °C and pH = 2. These adsorption results were used to validate the theoretical models by comparing both predicted and measured responses. Competitive adsorption was also carried out with a mixture of solutions composed of four molecules Caf, Tc, Pen, MB (initial concentration of 200 mg L^{-1}).

2.5.1. Kinetic study: Determination of equilibrium time

The kinetic study was carried out at 25 °C to evaluate the effect of the contact time of the AC_OP for the adsorption of pollutants. Thus, 20 mL of a Caf solution at 60 mg L^{-1} (at pH 6.4) were mixed with 10 mg of AC_OP for 5 to 240 min. For Tc, 20 mL of a 35 mg L^{-1} solution (at pH = 5.3) were mixed with 10 mg of AC_OP for 5 to 240 min. For Pen, 10 mL of a solution at 50 mg/L (at pH =5.6) were mixed with 10 mg of AC_OP for 10 to 2880 min.

2.5.2. Influence of initial pH value

The pH of the solutions was adjusted to 2, 4, 6, 8 and 10 by adding either NaOH (0.5 M) or HCl (0.5 M). For Caf, 25 mL of a 60 mg L^{-1} solution was mixed with 10 mg AC_OP and stirred for 3 h at 25 °C. For Tc, 20 mL of a 70 mg L^{-1} solution was mixed with 10 mg AC_OP and stirred for 3 h at 25 °C. For Pen, 10 mL of a 50 mg L^{-1} solution was mixed with 10 mg AC_OP and stirred for 12 h at 25 °C.

2.5.3. Influence of adsorption temperature

The influence of adsorption temperature was evaluated at 25, 30, 35 and 40 °C. The pH of all solutions was adjusted to an optimal value of pH 2 (determined in Section 2.5.2).

Caf solutions (25 mL at 60 mg L^{-1}) were placed in several bottles. Then, AC_OP (10 mg) was added to each bottle and the suspensions were stirred for 3 h at the desired temperature. Tc solutions (25 mL at 100 mg L^{-1}) were placed in several bottles. Then, AC_OP (10 mg) was added and the suspensions were shaken for 3 h at the desired temperature. Pen solutions (10 mL at 40 mg L^{-1}) were placed in several bottles. Then, AC_OP (10 mg) was added to each bottle and the suspensions were shaken for 12 h at the desired temperature.

2.5.4. Adsorption isotherms

The equilibrium adsorption isotherms were obtained using the optimal parameters determined in the kinetic tests (i.e. pH = 2 and $T = 25$ °C).

The experimental adsorption capacities at each time, q_e (mg g^{-1}), were calculated as follows in Eq. (3):

$$q_e = \frac{(C_0 - C_e)\,.V}{W} \tag{3}$$

where C_0 is the initial adsorbate concentration (mg L^{-1}), C_e is the adsorbate concentration at equilibrium (mg L^{-1}), V is the volume of adsorbate solution (mL) and W is the mass of adsorbent (g). Two models were used to fit the experimental data of adsorption using non-linear regression: the Langmuir model Eq. (4) and the Freundlich model Eq. (5).

$$q_e = \frac{q_L K_L C_e}{1 + K_L C_e} \tag{4}$$

$$q_e = K_F C_e^{1/n} \tag{5}$$

where q_e is the equilibrium adsorption capacity (mg g^{-1}) and C_e is the equilibrium solution concentration (mg L^{-1}). In Eq. (4), K_L represents the Langmuir adsorption constant (L mg^{-1}) and q_L indicates the Langmuir maximum adsorption capacity of the adsorbent. In Eq. (5), K_F represents the Freundlich isothermal constant (L g^{-1}); n indicates the Freundlich exponent called adsorbent intensity, which gives information on whether the adsorption process is favorable or not.

2.6. Textural characterization of ACs

Textural characterization of ACs were performed via N_2 sorption with a SORPTOMATIC series 1990 apparatus. Isotherm was recorded at 77 K, after outgassing the sample overnight at 250 °C. The specific surface area was determined from the adsorption branch using the Brunauer–Emmett–Teller (BET) equation model, at relative pressure of $P/P_0 = 0.22$. The zero charge point pH_{PZC} was determined and was measured when there is no change in pH after contact with the ACs. The procedure proposed by Boehm (1994) was used to determine the acid–base properties of the sample. Surface functionalization of ACs was evidenced by Fourier transform infrared spectroscopy (FT-IR spectrometer equipped with an ATR accessory, spectrum two PerkinElmer) using a resolution of 2 cm^{-1} in the range of 550–3500 cm^{-1}.

Scanning electron microscopy (SEM), observations, combined with energy dispersive X-ray (EDX) chemical analyses were performed with a HiVAC + VCD - Quanta 250 detector instrument (operated at 100 keV).

3. Results and discussion

3.1. Optimization analysis for each pollutant

3.1.1. Adsorption of caffeine (Caf)

ANOVA analysis (Table A.2) shows that the adsorption capacity of Caf increases considerably when raising the pyrolysis temperature from 600 °C to 800 °C (F value = 27.37) and the mass ratio precursor/acid from $r = 1.2$ to 2.5 (F value = 40.20). It can also be seen that extending the pyrolysis time allowed for a decrease of the adsorption capacity, although this effect was not statistically significant (Fig. A.1). The interaction between temperature and time ($T \times t$) indicates a negative effect on the adsorption of Caf, while a positive effect was found for the quadratic term of the acid/precursor ratio (r^2). Therefore, the mathematical model Y_1, represented by Eq. (6), only takes into account those terms with significant interactions (p-value < 0.05), in tandem with the time factor, even though its effect was marginal. High coefficient values of $R^2 = 0.929$ and R^2 adjusted = 0.887 were obtained, thus corroborating the model adequacy (Fig. 1A). Maximum Caf

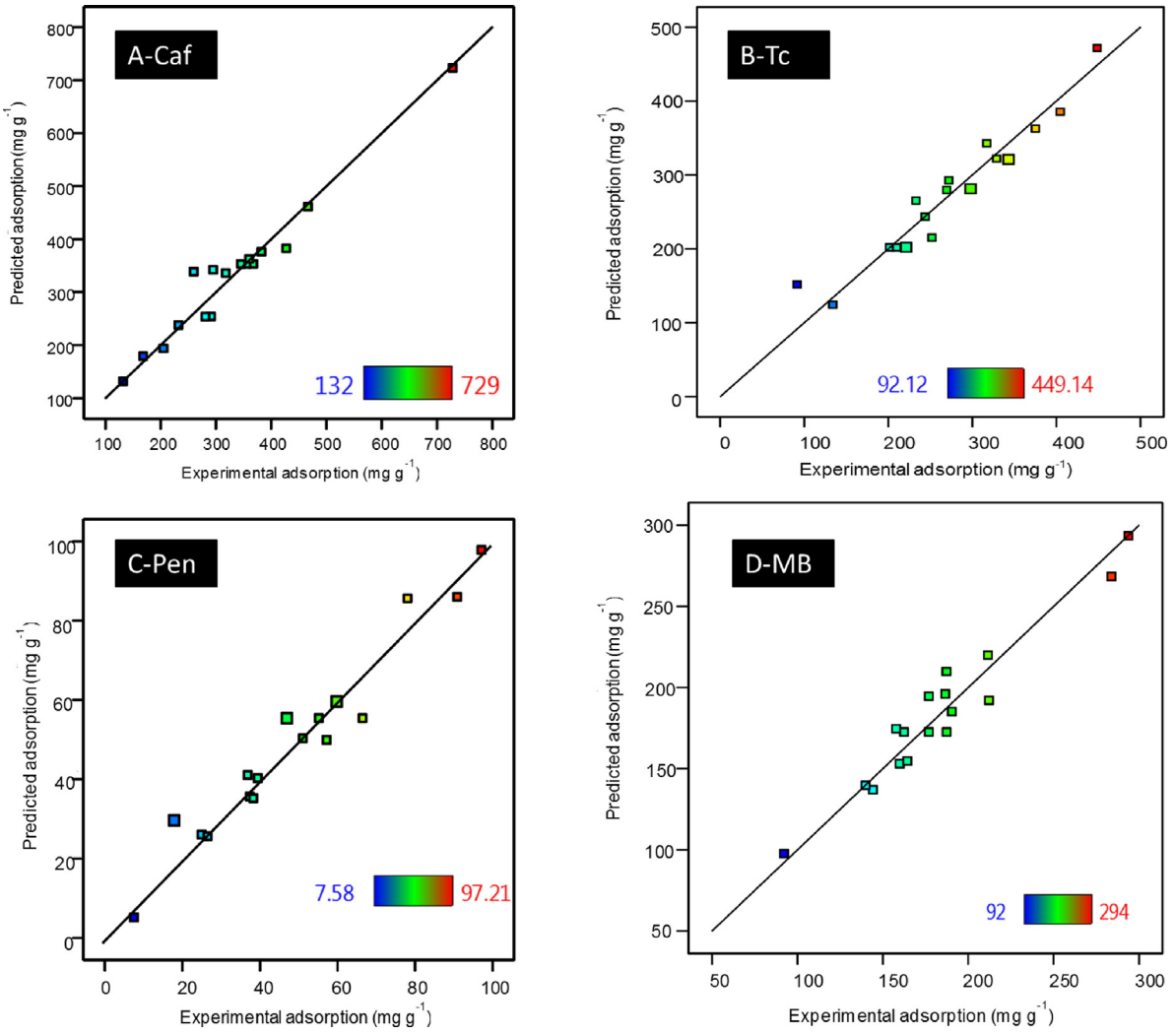

Fig. 1. Correlation between the actual and predicted adsorption of caffeine (A), tetracycline (B), penicillin (C) and methylene blue (D) on ACs. Colored inset bars represent the variation of adsorption values for each molecule.

adsorption capacity of 891 ± 64 mg/g was predicted by the quadratic model when utilizing an AC prepared at high temperature $T = 799$ °C, high $r = 2.5$ and $t = 60$ min.

$$Y_1 = -3220.6 + 6.4T - 417.0r + 25.6t + 182.2r^2 + 0.0997t^2 - 0.062T \times t \quad (6)$$

The model is graphically represented through response surface curves in Fig. 2(A) (B) (C), which illustrate the impact of factors variation on Caf adsorption. The parameters of the plot were set according to the optimal value of the effect of each factor. For a ratio ≥ 2 (Fig. 2(A) (C)), **t**here are two zones showing a high adsorption capacity of Caf: one at 120 min/600 °C, the other one at 60 min and at a high temperature of 800 °C. Fig. 2 (B) shows that for a fixed time of 60 min, the adsorption capacity is greater when using a high ratio and a very high temperature. Experimentally, a maximum adsorption capacity of 449.14 mg g^{-1} was obtained for AC prepared at $T = 600$ °C, $r = 0.5$ and $t = 120$ min (Table A.1). According to the experimental design, this AC was the one with the highest Caf adsorption capacity at the studied conditions. It is noteworthy to observe that in our previous study using similar ACs from *Sargassum (sp)*, a maximum Caf adsorption capacity of 221.61 mg g^{-1} was found (Francoeur et al., 2021). Such value is here doubled under optimized AC preparation conditions. Moreover, the predicted value can quadruple (from 221.61 to 891 mg g^{-1}), thereby giving confidence in the optimized results. A summary of adsorption capacity values of different biomass activated with H_3PO_4, is listed in Table 2.

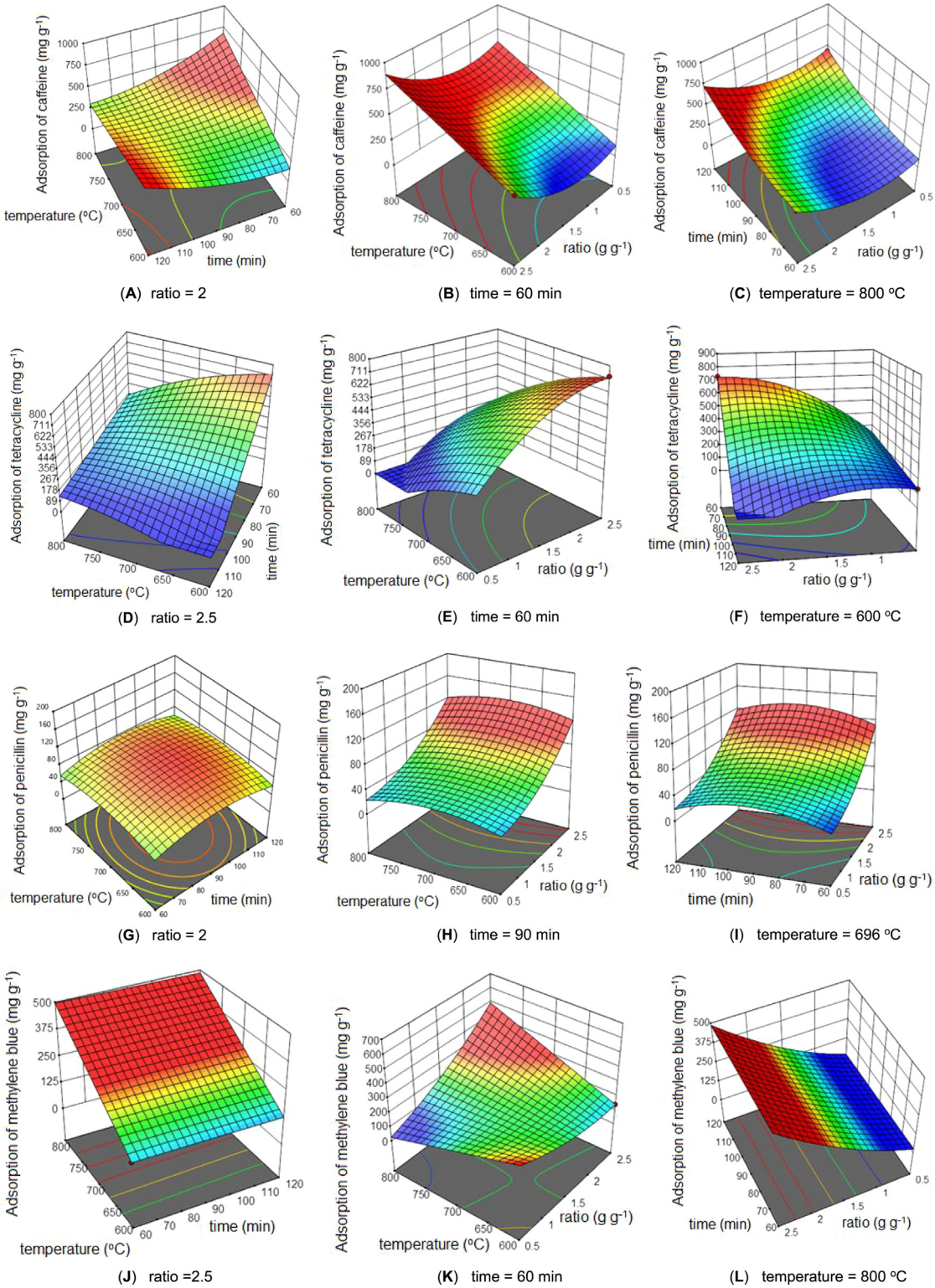

Fig. 2. Response surface showing the different effects of the preparation factors of activated carbon for the adsorption of pollutants : Temperature vs. Time (A) for Caf, (D) for Tc, (G) for Pen, (J) for MB; Temperature vs. Ratio (B) for Caf, (E) for Tc, (H) for Pen, (K) for MB; Time vs. Ratio (C) for Caf, (F) for Tc, (I) for Pen, (L) for MB.

Table 2
Summary of the capacity of adsorption of different biomass precursor activated with H_3PO_4.

Precursor	Activation	Adsorption capacity (mg/g)	References
Caffeine			
Sargassum (sp)	H_3PO_4 (85%) 1:1.25, 700 °C ,1 h 30 min	221.61	(Francoeur et al. 2021)
Sargassum (sp)	H_3PO_4 (85%) (H_3PO_4/precursor) 2.4, 664 °C,1 h 5 min	329	This study
Sargassum (sp)	H_3PO_4 (85%) (H_3PO_4/precursor) 0.5, 600 °C, 2 h	449.14	This study
Tetracycline			
Peach stone	H_3PO_4 (85%), 400 °C, 4 h	845.9	(Álvarez-Torrellas et al. 2016)
Corn straw	H_3PO (85%) (H_3PO_4/precursor) 1, 300 °C	227.3	(Yang et al. 2020)
Sargassum (sp)	H_3PO_4 (85%) (H_3PO_4/precursor) 2.5, 600 °C, 1 h	729	This study
Sargassum (sp)	H_3PO_4 (85%) (H_3PO_4/precursor) 2.4, 664 °C, 1 h 5 min	579.69	This study
Penicillin			
Sargassum (sp)	H_3PO_4 (85%) (H_3PO_4/precursor) 2.4, 664 °C, 1 h 5 min	97.21	This study
Methylene Blue			
Vetiver roots	H_3PO_4 (85%) (H_3PO_4/precursor) 1.5:1, 600 °C, 1 h	423	(Altenor et al. 2009)
Coconut leaves	H_3PO_4 (85%)	357.14	(Jawad et al. 2017)
Sargassum (sp)	H_3PO_4 (85%) (H_3PO_4/precursor) 2.4, 664 °C ,1 h 5 min	294	This study

3.1.2. Tetracycline (Tc) adsorption

The ANOVA calculations for the quadratic Tc adsorption model, displayed in Table A.3, shows that the AC adsorption capacity decreases with increasing both pyrolysis temperature T and pyrolysis time t. It can also be seen that the adsorption capacity increases with increasing ratio (Fig. A.2).

The interaction between temperature and time ($T \times t$) shows a positive effect (F value = 32.09) on the adsorption of Tc, while the interaction acid/precursor ratio × time ($r \times t$) significantly decreases the adsorption capacity of the AC.

After suppression of non-significant terms, a relationship between Tc adsorption and the coded parameters was expressed by Eq. (7). The coefficients values $R^2 = 0.9541$ and R^2 adjusted = 0.9184 indicate that this model can be used for very good prediction of Tc adsorption (Fig. 1B).

$$Y_2 = 826.1 + 1.79T + 972.9r - 35.5t - 121.2r^2 - 0.0055T^2 + 0.061T \times t - 6.2r \times t \quad (7)$$

Model Y_2 predicts an optimal adsorption value of 722 ± 39 mg g^{-1} when preparing AC at $T = 600$ °C, $r = 2.4$ and $t = 60$ min.

The effects of the variation of the factors on Tc adsorption are shown by the surface curves in Fig. 2(D) (E) (F). For a mass ratio $r = 2.5$, a greater adsorption zone is observed at short pyrolysis time ($t = 60$ min) and lower temperature ($T = 600$ °C). It can also be noted that unlike Caf, a pyrolysis carried out at very high temperature and a low ratio, does not facilitate the adsorption of Tc since the adsorption capacity tends to zero.

Experimentally, Tc adsorption capacity reached a value of 729 mg g^{-1} for AC prepared at $T = 600$ °C $r = 2.5$ and $t = 60$ min, against 722 mg g^{-1} predicted by Y_2. This value was the highest in the experimental design data (Table A.1). Adsorption capacities values of Tc on activated carbons prepared with H_3PO_4 from peach pit and corn straw of 845.9 mg g^{-1} (Álvarez-Torrellas et al., 2016) and 227.3 mg g^{-1} (Yang et al., 2020), respectively, have been reported. When comparing Tc adsorption capacity values of those lignocellulosic precursors, one can note that *Sargassum* derived ACs exhibit good performance, thereby providing a promising alternative to produce low-cost carbon-based sorbents.

3.1.3. Penicillin (Pen) adsorption

The results of the ANOVA for Pen adsorption on different ACs (Table A.4) show that Pen adsorption decreases substantially with the increase of the acid/precursor mass ratio (F value of 148.51). In addition, the mass ratio is the only factor that has a significant effect on the variation of Pen adsorption on ACs (Fig. A.3).

The interactions of the quadratic terms of temperature (T^2) and time (t^2) show significant negative effects, while the quadratic term of acid/precursor ratio (r^2) promotes the increase in the response variable.

The mathematical model established for Pen adsorption is represented by Eq. (8). With coefficients values R^2 of 0.9481 and R^2 adjusted of 0.9169, this model gives a very good prediction for Pen adsorption on *Sargassum* derived AC (Fig. 1C).

$$Y_3 = -790.4 + 1.94T - 51.8\mathrm{r} + 3.83t + 26.6r^2 - 0.022t^2 + 0.26r \times t - 0.0014T^2 \quad (8)$$

The optimal value of Pen adsorption capacity using the AC prepared at $T = 686$ °C, $r = 2.5$ and $t = 99$ min was of 146 ± 7 mg/g.

The response surface curves (Fig. 2(G) (H) (I)) show the influence of the acid/precursor mass ratio on the variation of Pen adsorption. Two distinct regions can thus be seen: a region of the response surface for a low adsorption capacity ($r < 2$) and another region of very high adsorption capacity for $r \geq 2$.

Experimentally, an adsorption capacity of 97.21 mg/g was found for AC prepared at $T = 600$ °C, $r = 2.5$ and $t = 60$ min against 97 mg/g predicted (Table A.1). This AC had the highest adsorption capacity for Pen in the experimental design.

3.1.4. Adsorption of methylene blue (MB)

The AVOVA analysis depicted in Table A.5 shows that MB adsorption highly increases with both T and r, while the parameter t had no effect (Fig. A.4).

The interaction between the temperature and the ratio ($T \times r$) shows extremely high effects (F value of 125.62). With $R^2 = 0.9342$ and R^2 adjusted $= 0.9043$, the mathematical model Y_4 given by Eq. (9) had a high degree of prediction and was used for the MB adsorption (Fig. 1C).

$$Y_4 = 1715.9 - 2.17T - 1174r - 0.16t + 1.58T \times r + 47.9r^2 \quad (9)$$

The model Eq. (9) predicts an optimal value of 492 ± 37 mg g^{-1} for the adsorption capacity of MB on the AC prepared at $T = 799$ °C, $r = 2.5$ and $t = 69$ min.

With almost flat surface curves, certain linearity can be observed in the increase of the MB adsorption capacity in relation with the variation of the acid/precursor mass ratio (Fig. 2 (J) (K) (L)). However, the increase is more pronounced for r >1.5.

An adsorption capacity of 294 mg/g was obtained in the experiments for AC which was prepared at $T = 600$ °C, $r = 2.5$ and $t = 120$ min, against the 293 mg/g predicted. The MB adsorption capacities for other biomasses impregnated with H_3PO_4 such as Vetiver root, coconut and pine needle biomass of 423 mg g^{-1} (Altenor et al., 2009) and 357 mg g^{-1} (Jawad et al., 2017) 154 mg g^{-1} (Pandey et al., 2022), respectively, have been reported. El Maguana et al. published in an optimization study for the preparation of AC from nut cake, that the MB adsorption capacity could range from 70.39 to 243.04 mg g^{-1} (El Maguana et al., 2018).

3.1.5. Desirability analysis

The objective of the experimental design in this study was to evaluate the optimal conditions for the preparation of AC with improved removal efficiency for the four pollutants tested. The analysis of the global desirability D= 0.93 showed a better condition of preparation of AC with better capacity for the adsorption for all pollutants tested. From this, the AC should be prepared with a pyrolysis temperature $T = 664$ °C, a mass ratio (H_3PO_4/precursor) $r = 2.4$ and a pyrolysis time $t = 65$ minutes. Therefore, this optimal AC (herein labeled AC_OP) was produced and retained for additional adsorption measurements.

The prediction of the adsorption capacities of this AC_OP were as follows: 329 ± 28 mg g^{-1} for Caf, 150 ± 7 mg g^{-1} for Pen, 579 ± 39 mg g^{-1} for Tc and 223 ± 14 mg g^{-1} for MB (Table A.1).

3.2. Textural characterization of ACs

The statistical analysis carried out previously showed that the adsorption capacities of the ACs could vary significantly when the experimental synthesis conditions are modified.

We also sought to evaluate the impact of synthesis conditions on AC production yield. As a reminder, the AC production yield is defined as the ratio between the weight of AC (after activation, washing and drying) and the weight of the precursor. The influence of the quantitative parameters r, T and t on the yield of *Sargassum*-based ACs is presented in Fig. A.5. For *Sargassum* AC, it can be seen that the yield decreases with increasing acid/precursor mass ratio, pyrolysis time and temperature (R^2 of 0.7 for a quadratic model) (Fig. A.5). This decrease is due to the loss of volatile matter with increasing pyrolysis temperature. The yield varies very significantly with the variation of r, since with a high phosphoric acid content, gasification of the surface carbon atoms becomes predominant (Patnukao and Pavasant, 2008; Yorgun and Yıldız, 2015). The production yield of AC from *Sargassum* varies between 24% and 33%.

The specific surface measurements of *Sargassum* based ACs (Table A.1) show a quadratic correlation as a function of the preparation parameters with a very good prediction ($R^2 = 0.91$). Only the interaction between temperature and time seems to have a significant effect on the BET surface (Fig. A.6). The BET surface value predicted by the model (BET = 570.3 - 438.7T + 23.8r + 373t + 659.6Tt + 345T^2) for AC_OP (Fig. A.8) is 934 m^2 g^{-1} against 929 m^2 g^{-1} measured. The optimal BET surface area predicted would be 1005 ± 163 m^2 g^{-1} for AC prepared at 634 °C, a mass ratio of 2.5 during 120 min of pyrolysis.

The FT-IR analysis shows that all ACs have the same surface groups (Fig. A.7). Only the concentration of acidic or basic groups differs depending on the conditions of AC preparation. No correlation could be found between synthesis conditions and the measured surface groups or the pHpzc of the ACs. The concentration of the groups also depends on the washing method used to obtain ACs.

As shown in the FTIR spectra (Fig. A.7), the peak at about 870 cm^{-1} is associated with the structure of the out-of-plane bending vibration of the aromatic C–H; the peak between 1100–1050 cm^{-1} is attributed to C-OH group; the peak at 1250–1200 cm^{-1} can be attributed to the hydrogen-bonded P=O stretching mode, to the O–C stretching vibrations in the P–O–C, and P=OOH bond; the peak between 1600–1500 cm^{-1} is characteristic to C–N vibrations and at 1700 cm^{-1} to C=N; the peak at 2300 cm^{-1} can be assigned to P-H; and the peak between 3000–2900 cm^{-1} is attributed to O–C=O. It must be underlined that the XPS analysis of raw *Sargassum* also showed the presence of phosphorus species. Phosphocarbonaceous groups were also found in other algae AC activated with H_3PO_4 (Yacou et al., 2018). The XPS analyses showed that ACs contain elements such as N (0.83–1.89%), P (1.8–5.62%) which are consistent with the detection of C=N, C–N and P=O bonds in FTIR, bonds that provide the AC basic character.

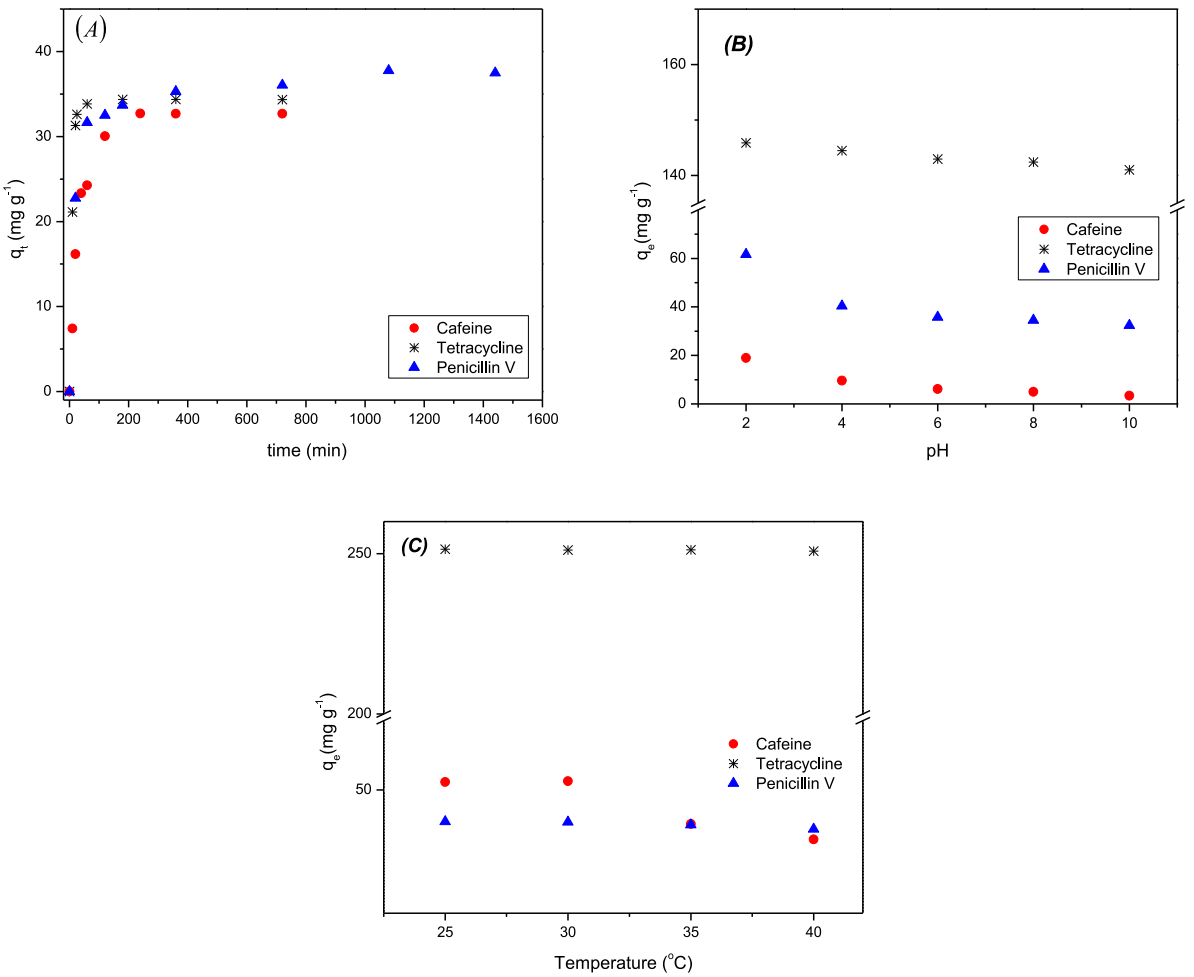

Fig. 3. The effect of contact time (A), pH (B) and temperature (C) on the removal efficiency of Caf, Tc and Pen (initial concentrations 60, 35 and 50 mg/L· respectively) using AC_OP.

The surface elemental composition of AC_OP determined by EDX analysis, shows various elements such as O, P, Ca and S, which are in consistent with the previous XPS and FTIR analyses.

The pHpzc measurements as well as the quantification of the surface groups by the Boehm's method show that all ACs have more acidic properties (Table A.1). The pHpzc decreases with increasing acid/precursor mass ratio until the r=1.5, then the pHpzc increases with increasing r. The same trend is observed with the pyrolysis time.

3.3. Kinetic and isotherm adsorption studies on the optimum activated carbon (AC_OP)

After identifying the optimum conditions, AC_OP was prepared in order to verify (i) the accuracy of the models obtained (by comparing the experimental and predicted values), and (ii) to study the effect of additional parameters such as contact time, pH and temperature on the adsorption.

As shown in Fig. 2, adequacy of the models Y_1, Y_2, Y_3 and Y_4 was verified by measuring maximum adsorption capacities of the AC_OP as follows: for Caf = 329.04 mg g^{-1}, Tc = 579.69 mg g^{-1}, Pen = 150.34 mg g^{-1}, MB = 222.62 mg g^{-1} (with 95% confidence interval). The predicted values of the adsorption capacity of this AC were for Tc = 572 ± 39 mg g^{-1}, Caf = 473 ± 28 mg g^{-1}, MB = 243 ± 14 mg g^{-1} and Pen = 110 ± 7 mg g^{-1} (Table A.6). Interestingly, the descending order for those actual measurements (i.e. Tc > Caf > MB > Pen) was similar to that of predicted values, hence confirming the models accuracy.

Three pharmaceutical compounds (i.e. Caf, Tc and Pen) were selected to perform adsorption kinetic studies on AC_OP. Fig. 3A shows the influence of the contact time on the adsorption capacity of AC_OP for the three pollutants. Both adsorption kinetics of Caf and Tc are relatively fast with equilibrium times reached before 3 h for Caf (pseudo second order kinetics, R^2 = 0.983, K_2 = 0.0467) and 30 min for Tc (pseudo second order kinetics, R^2 = 0.999, K_2 = 3.163).

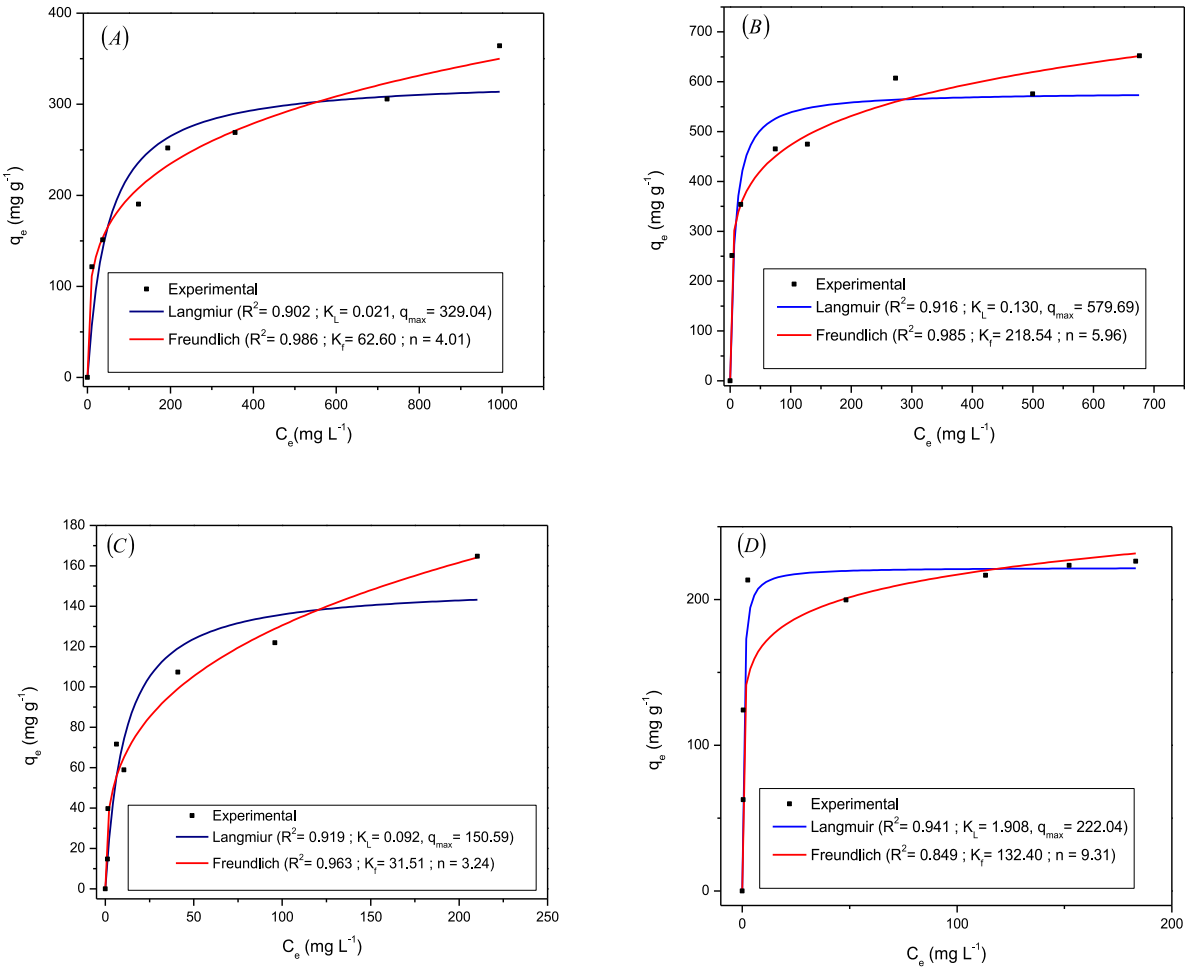

Fig. 4. Adsorption curves with fitted isotherm models (Langmuir and Freundlich) at 25 °C and pH 2: (A) Caf for 3 h; (B) Tc for 3 h; (C) Pen for 12 h; (D) MB for 3 h.

Such result agrees with observations from other studies, which reported values for equilibrium time for Caf adsorption on AC ranging from 1.5 to 4 h, depending on the testing conditions (Beltrame et al., 2018; Francoeur et al., 2021; Torrellas et al., 2015). For Tc, values ranging from 0.5 to 4 h are usually reported (Choi et al., 2020; Fan et al., 2016); but adsorption equilibrium can be reached later depending on the activated carbon used (Álvarez-Torrellas et al., 2016; Yang et al., 2020; Li et al., 2013). In this study, 3 h contact time was chosen, although equilibrium was reached before 1 h. By contrast, Pen gives very slow adsorption kinetics with equilibrium reached after 12 h (pseudo second order kinetics, $R^2 = 0.999$, $K_2 = 0.0317$) (see Fig. 3C).

When increasing the pH, the pollutants adsorption capacity on AC_OP decreases as observed in literature for other ACs (Francoeur et al., 2021; Pouretedal and Sadegh, 2014). The optimum pH is 2 as shown in the curves in Fig. 3B. Other studies show that the optimal pH is one in an acidic environment (Li et al., 2013; Huang et al., 2014; Reis et al., 2020; Melo et al., 2020). Fig. 4 shows the curves of the non-linear Langmuir and Freundlich models Eq. (4) and Eq. (5) isotherms fitting the experimental data of the Caf, Tc, Pen and MB adsorption on AC_OP at 25 °C and pH 2. The Freundlich model is best suited for the adsorption of Caf, Tc, Pen and the Langmuir model for the adsorption of MB.

Competitive adsorption for the quaternary system, (i.e. with all four molecules added simultaneously), showed that total pollutant removal decreases in the following order : MB >Tc > Caf > Pen with values of 70.8%, 48.9%, 39.9% and 39.7%, respectively (Fig. 5).

Effective removing of tetracycline, penicillin, caffeine, and methylene blue from contaminated wastewater on activated carbon that has been synthesized from *Sargassum (sp)* shows that the invasive brown algae, causing seriously problems in many part around the world the Caribbean, can be valorized as an inexpensive raw material for the synthesis of activated carbon for wastewater treatment.

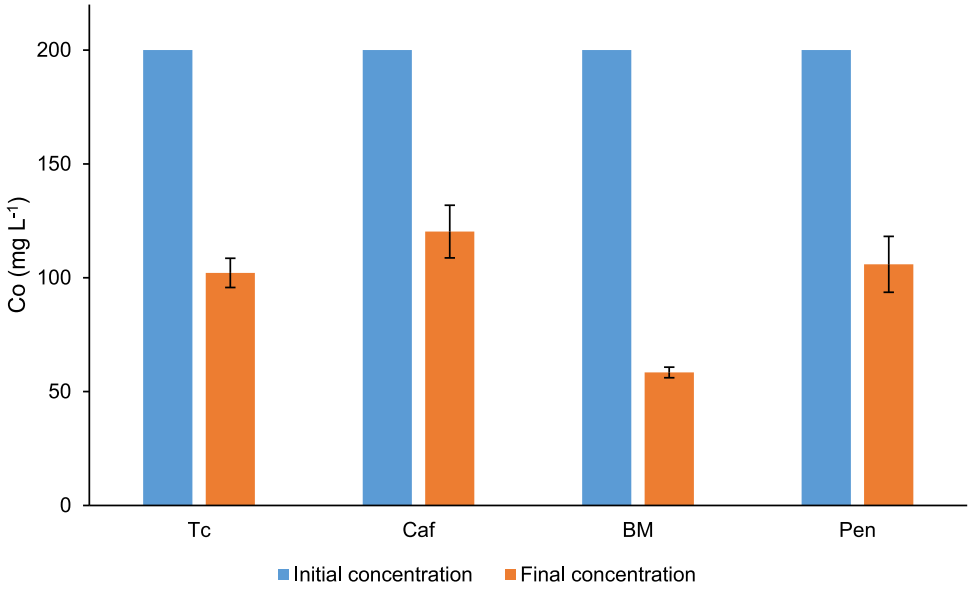

Fig. 5. Competitive adsorption for quaternary systems with four molecules added simultaneously at 25 °C and pH 5 for 24 H with 200 mg L^{-1} of each molecules.

4. Conclusions

In this work, the optimization of the production of activated carbon from an invasive biomass *Sargassum (sp.)* has been accomplished. The optimal conditions for preparing the AC were: acid/precursor mass ratio of 2.4 during 65 min of pyrolysis at 664 °C. Batch adsorption isotherms on this AC showed an adsorption capacity of 329, 579, 150 and 222 mg g^{-1} for Caf, Tc, Pen and MB, respectively, at acid pH = 2. For a mixture with four molecules at 200 mg L^{-1} each, the optimal AC adsorbs 39.9%, 48.9%, 39.7% and 70.8% of Caf, Tc, Pen and MB, respectively. These results provide new knowledge on the possibilities of valorizing *Sargassum (sp)* algae for pollutants adsorption in wastewaters. However, further study of stability and reusability of the material needs to be carried out on real wastewater to confirm the results obtained.

E-supplementary data of this work can be found in online version of the paper

CRediT authorship contribution statement

Marckens Francoeur: Data curation, Methodology, Formal analysis, Validation, Visualization, Writing – original draft. **Christelle Yacou:** Writing – review & editing. **Corine Jean-Marius:** Resources. **Yvens Chérémond:** Writing – review & editing. **Ulises Jauregui-Haza:** Writing – review & editing. **Sarra Gaspard:** Writing – review & editing, Supervision.

Declaration of competing interest

The authors declare that they have no known competing financial interests or personal relationships that could have appeared to influence the work reported in this paper.

Data availability

Data will be made available on request.

Acknowledgments

The authors wish to thank the financial support for this work provided by the Cooperation Service of the French Embassy in Haïti and The Université Publique du Sud-Est à Jacmel.

Appendix A. Supplementary data

Supplementary material related to this article can be found online at https://doi.org/10.1016/j.eti.2022.102940.

References

Ahmed, M.B., Zhou, J.L., Ngo, H.H., Guo, W., 2015. Adsorptive removal of antibiotics from water and wastewater: Progress and challenges. Sci. Total Environ. 532, 112–126. http://dx.doi.org/10.1016/j.scitotenv.2015.05.130.

Ali, M.E.M., Abd El-Aty, A.M., Badawy, M.I., Ali, R.K., 2018. Removal of pharmaceutical pollutants from synthetic wastewater using chemically modified biomass of green alga scenedesmus obliquus. Ecotoxicol. Environ. Saf. 151, 144–152. http://dx.doi.org/10.1016/j.ecoenv.2018.01.012.

Altenor, S., Carene, B., Emmanuel, E., Lambert, J., Ehrhardt, J.-J., Gaspard, S., 2009. Adsorption studies of methylene blue and phenol onto vetiver roots activated carbon prepared by chemical activation. J. Hazard. Mater. 165, 1029–1039. http://dx.doi.org/10.1016/j.jhazmat.2008.10.133.

Álvarez-Torrellas, S., Rodríguez, A., Ovejero, G., García, J., 2016. Comparative adsorption performance of ibuprofen and tetracycline from aqueous solution by carbonaceous materials. Chem. Eng. J. 283, 936–947. http://dx.doi.org/10.1016/j.cej.2015.08.023.

Anon, 2021. Removal of tetracycline from wastewater using magnetic biochar: A comparative study of performance based on the preparation method. Environ. Technol. Innov. 24, 101916. http://dx.doi.org/10.1016/j.eti.2021.101916.

Barquilha, C.E.R., Cossich, E.S., Tavares, C.R.G., Silva, E.A., 2019. Biosorption of nickel(II) and copper(II) ions by Sargassum sp, in nature and alginate extraction products. Bioresour. Technol. Rep. 5, 43–50. http://dx.doi.org/10.1016/j.biteb.2018.11.011.

Beltrame, K.K., Cazetta, A.L., de Souza, P.S.C., Spessato, L., Silva, T.L., Almeida, V.C., 2018. Adsorption of caffeine on mesoporous activated carbon fibers prepared from pineapple plant leaves. Ecotoxicol. Environ. Saf. 147, 64–71. http://dx.doi.org/10.1016/j.ecoenv.2017.08.034.

Boehm, H.P., 1994. Some aspects of the surface chemistry of carbon blacks and other carbons. Carbon 32, 759–769. http://dx.doi.org/10.1016/0008-6223(94)90031-0.

Capodaglio, A.G., 2020. Critical perspective on advanced treatment processes for water and wastewater: AOPs, ARPs, and AORPs. Appl. Sci. (Switzerland) 10, http://dx.doi.org/10.3390/app10134549.

Carvalho, I.T., Santos, L., 2016. Antibiotics in the aquatic environments: A review of the European scenario. Environ. Int. 94, 736–757. http://dx.doi.org/10.1016/j.envint.2016.06.025.

Chaturvedi, P., Shukla, P., Giri, B.S., Chowdhary, P., Chandra, R., Gupta, P., Pandey, A., 2021. Prevalence and hazardous impact of pharmaceutical and personal care products and antibiotics in environment: A review on emerging contaminants. Environ. Res. 194, 110664. http://dx.doi.org/10.1016/j.envres.2020.110664.

Choi, Y.-K., Choi, T.-R., Gurav, R., Bhatia, S.K., Park, Y.-L., Kim, H.J., Kan, E., Yang, Y.-H., 2020. Adsorption behavior of tetracycline onto *spirulina sp*, (*microalgae*)-derived biochars produced at different temperatures. Sci. Total Environ. 710, 136282. http://dx.doi.org/10.1016/j.scitotenv.2019.136282.

de S. Coração, A.C., dos Santos, F.S., Duarte, J.A.D., Lopes-Filho, E.A.P., De-Paula, J.C., Rocha, L.M., Krepsky, N., Fiaux, S.B., Teixeira, V.L., 2020. What do we know about the utilization of the Sargassum species as biosorbents of trace metals in Brazil? J. Environ. Chem. Eng. 8, 103941. http://dx.doi.org/10.1016/j.jece.2020.103941.

El Maguana, Y., Elhadiri, N., Bouchdoug, M., Benchanaa, M., 2018. Study of the influence of some factors on the preparation of activated carbon from walnut cake using the fractional factorial design. J. Environ. Chem. Eng. 6, 1093–1099. http://dx.doi.org/10.1016/j.jece.2018.01.023.

Esmaeili, A., Ghasemi, S., Rustaiyan, A., 2010. Removal of hexavalent chromium using activated carbons derived from marine algae gracllaria and sargassum sp. J. Mar. Sci. Technol. 18, 587–592.

Fan, H.-T., Shi, L.-Q., Shen, H., Chen, X., Xie, K.-P., 2016. Equilibrium, isotherm, kinetic and thermodynamic studies for removal of tetracycline antibiotics by adsorption onto hazelnut shell derived activated carbons from aqueous media. RSC Adv. 6, 109983–109991. http://dx.doi.org/10.1039/C6RA23346E.

Franco, J., 2008. Planification d'expériences numériques en phase exploratoire pour la simulation des phénomènes complexes, phdthesis, Ecole Nationale Supérieure des Mines de Saint-Etienne. https://tel.archives-ouvertes.fr/tel-00803107. (Accessed 18 February 2020).

Francoeur, M., Ferino-Pérez, A., Yacou, C., Jean-Marius, C., Emmanuel, E., Chérémond, Y., Jauregui-Haza, U., Gaspard, S., 2021. Activated carbon synthetized from sargassum (sp) for adsorption of caffeine: Understanding the adsorption mechanism using molecular modeling. J. Environ. Chem. Eng. 9, 104795. http://dx.doi.org/10.1016/j.jece.2020.104795.

He, J., Chen, J.P., 2014. A comprehensive review on biosorption of heavy metals by algal biomass: Materials, performances, chemistry, and modeling simulation tools. Bioresour. Technol. 160, 67–78. http://dx.doi.org/10.1016/j.biortech.2014.01.068.

Homem, V., Santos, L., 2011. Degradation and removal methods of antibiotics from aqueous matrices - A review. J. Environ. Manage. http://dx.doi.org/10.1016/j.jenvman.2011.05.023.

Huang, L., Wang, M., Shi, C., Huang, J., Zhang, B., 2014. Adsorption of tetracycline and ciprofloxacin on activated carbon prepared from lignin with H3Po4 activation. Desalination Water Treat. 52, 2678–2687. http://dx.doi.org/10.1080/19443994.2013.833873.

Jawad, A.H., Rashid, R.A., Ismail, K., Sabar, S., 2017. High surface area mesoporous activated carbon developed from coconut leaf by chemical activation with H3PO4 for adsorption of methylene blue. Desalination Water Treat. 74, 326–335, https://www.cabdirect.org/cabdirect/abstract/20173275270. (Accessed 21 January 2021).

Krasucka, P., Pan, B., Sik Ok, Y., Mohan, D., Sarkar, B., Oleszczuk, P., 2021. Engineered biochar – A sustainable solution for the removal of antibiotics from water. Chem. Eng. J. 405, 126926. http://dx.doi.org/10.1016/j.cej.2020.126926.

Krishnan, R.Y., Manikandan, S., Subbaiya, R., Biruntha, M., Govarthanan, M., Karmegam, N., 2021. Removal of emerging micropollutants originating from pharmaceuticals and personal care products (PPCPs) in water and wastewater by advanced oxidation processes: A review. Environ. Technol. Innov. 23, 101757. http://dx.doi.org/10.1016/j.eti.2021.101757.

Levy, S.B., Bonnie, M., 2004. Antibacterial resistance worldwide: Causes, challenges and responses. Nat. Med. 10, S122–S129. http://dx.doi.org/10.1038/nm1145.

Li, S., Wang, X., Tan, S., Shi, Y., Li, W., 2017. CrO3 supported on sargassum-based activated carbon as low temperature catalysts for the selective catalytic reduction of NO with NH3. Fuel. 191, 511–517. http://dx.doi.org/10.1016/j.fuel.2016.11.095.

Li, G., Zhang, D., Wang, M., Huang, J., Huang, L., 2013. Preparation of activated carbons from Iris tectorum employing ferric nitrate as dopant for removal of tetracycline from aqueous solutions. Ecotoxicol. Environ. Saf. 98, 273–282. http://dx.doi.org/10.1016/j.ecoenv.2013.08.015.

Ma, Y., Li, P., Yang, L., Wu, L., He, L., Gao, F., Qi, X., Zhang, Z., 2020. Iron/zinc and phosphoric acid modified sludge biochar as an efficient adsorbent for fluoroquinolones antibiotics removal. Ecotoxicol. Environ. Saf. 196, 110550. http://dx.doi.org/10.1016/j.ecoenv.2020.110550.

Mansas, C., Mendret, J., Brosillon, S., Ayral, A., 2020. Coupling catalytic ozonation and membrane separation: A review. Sep. Purif. Technol. 236, 116221. http://dx.doi.org/10.1016/j.seppur.2019.116221.

Mathieu, D., Phan-Tan-Luu, R., 2001. Planification d'expériences en formulation : optimisation. p. 21, https://www.techniques-ingenieur.fr/res/pdf/encyclopedia/42611210-j2241.pdf.

Melo, L.L.A., Ide, A.H., Duarte, J.L.S., Zanta, C.L.P.S., Oliveira, L.M.T.M., Pimentel, W.R.O., Meili, L., 2020. Caffeine removal using elaeis guineensis activated carbon: adsorption and RSM studies. Environ. Sci. Pollut. Res. 27, 27048–27060. http://dx.doi.org/10.1007/s11356-020-09053-z.

Pandey, D., Daverey, A., Dutta, K., Yata, V.K., Arunachalam, K., 2022. Valorization of waste pine needle biomass into biosorbents for the removal of methylene blue dye from water: Kinetics, equilibrium and thermodynamics study. Environ. Technol. Innov. 25, 102200. http://dx.doi.org/10.1016/j.eti.2021.102200.

Patnukao, P., Pavasant, P., 2008. Activated carbon from Eucalyptus camaldulensis Dehn bark using phosphoric acid activation. Bioresour. Technol. 99, 8540–8543. http://dx.doi.org/10.1016/j.biortech.2006.10.049.

Phoon, B.L., Ong, C.C., Mohamed Saheed, M.S., Show, P.-L., Chang, J.-S., Ling, T.C., Lam, S.S., Juan, J.C., 2020. Conventional and emerging technologies for removal of antibiotics from wastewater. J. Hazard. Mater. 400, http://dx.doi.org/10.1016/j.jhazmat.2020.122961.

Pinteus, S., Lemos, M.F.L., Alves, C., Neugebauer, A., Silva, J., Thomas, O.P., Botana, L.M., Gaspar, H., Pedrosa, R., 2018. Marine invasive macroalgae: Turning a real threat into a major opportunity - the biotechnological potential of Sargassum muticum and Asparagopsis armata. Algal Res. 34, 217–234. http://dx.doi.org/10.1016/j.algal.2018.06.018.

Pouretedal, H.R., Sadegh, N., 2014. Effective removal of amoxicillin, cephalexin, tetracycline and penicillin G from aqueous solutions using activated carbon nanoparticles prepared from vine wood. J. Water Process Eng. 1, 64–73. http://dx.doi.org/10.1016/j.jwpe.2014.03.006.

Radaei, E., Alavi Moghaddam, M.R., Arami, M., 2014. Removal of reactive blue 19 from aqueous solution by pomegranate residual-based activated carbon: optimization by response surface methodology. J. Environ. Health Sci. Eng. 12, 65. http://dx.doi.org/10.1186/2052-336X-12-65.

Reis, A.C., Kolvenbach, B.A., Nunes, O.C., Corvini, P.F.X., 2020. Biodegradation of antibiotics: The new resistance determinants – part II. New Biotechnol. 54, 13–27. http://dx.doi.org/10.1016/j.nbt.2019.08.003.

Rivas, J., Encinas, Á., Beltrán, F., Graham, N., 2011. Application of advanced oxidation processes to doxycycline and norfloxacin removal from water. J. Environ. Sci. Health A 46, 944–951. http://dx.doi.org/10.1080/10934529.2011.586249.

Tayo, L.L., Caparanga, A.R., Doma, B.T., Liao, C.-H., 2018. A review on the removal of pharmaceutical and personal care products (PPCPs) using advanced oxidation processes. J. Adv. Oxid. Technol. 21, http://dx.doi.org/10.26802/jaots.2017.0079.

Torrellas, S.Á., García Lovera, R., Escalona, N., Sepúlveda, C., Sotelo, J.L., García, J., 2015. Chemical-activated carbons from peach stones for the adsorption of emerging contaminants in aqueous solutions. Chem. Eng. J. 279, 788–798. http://dx.doi.org/10.1016/j.cej.2015.05.104.

Wang, J., Zhuan, R., Chu, L., 2019. The occurrence, distribution and degradation of antibiotics by ionizing radiation: An overview. Sci. Total Environ. 646, 1385–1397. http://dx.doi.org/10.1016/j.scitotenv.2018.07.415.

Yacou, C., Altenor, S., Carene, B., Gaspard, S., 2018. Chemical structure investigation of tropical Turbinaria turbinata seaweeds and its derived carbon sorbents applied for the removal of hexavalent chromium in water. Algal Res. 34, 25–36. http://dx.doi.org/10.1016/j.algal.2018.06.014.

Yang, Q., Wu, P., Liu, J., Rehman, S., Ahmed, Z., Ruan, B., Zhu, N., 2020. Batch interaction of emerging tetracycline contaminant with novel phosphoric acid activated corn straw porous carbon: Adsorption rate and nature of mechanism. Environ. Res. 181, 108899. http://dx.doi.org/10.1016/j.envres.2019.108899.

Yorgun, S., Yıldız, D., 2015. Preparation and characterization of activated carbons from paulownia wood by chemical activation with H3Po4. J. Taiwan Inst. Chem. Eng. 53, 122–131. http://dx.doi.org/10.1016/j.jtice.2015.02.032.